

The effect of dexamethasone/cell-penetrating peptide nanoparticles on gene delivery for inner ear therapy

Ji Young Yoon¹
Keum-Jin Yang²
Shi-Nae Park³
Dong-Kee Kim³
Jong-Duk Kim¹

¹Department of Chemical and Biomolecular Engineering, BK 21 Plus Program, Korea Advanced Institute of Science and Technology, Guseong-Dong, Yuseong-Gu, Daejeon, ²Clinical Research Institute, St Mary's Hospital, Daejeon, ³Department of Otolaryngology – Head and Neck Surgery, College of Medicine, The Catholic University of Korea, Seoul, Republic of Korea

Correspondence: Dong-Kee Kim
Department of Otolaryngology – Head and Neck Surgery, College of Medicine, The Catholic University of Korea, 222, Banpo-daero, Seocho-gu, Seoul (06591), Republic of Korea
Tel +82 10 3296 5204
Email cider12@catholic.ac.kr

Jong-Duk Kim
Department of Chemical and Biomolecular Engineering, Korea Advanced Institute of Science and Technology, 291, Daehak-ro, Yuseong-gu, Daejeon, Republic of Korea
Tel +82 10 9484 3921
Email kjd@kaist.ac.kr

Abstract: Dexamethasone (Dex)-loaded PHEA-g-C18-Arg8 (PCA) nanoparticles (PCA/Dex) were developed for the delivery of genes to determine the synergistic effect of Dex on gene expression. The cationic PCA nanoparticles were self-assembled to create cationic micelles containing an octadecylamine (C18) core with Dex and an arginine 8 (Arg8) peptide shell for electrostatic complexation with nucleic acids (connexin 26 [Cx26] siRNA, green fluorescent protein [GFP] DNA or brain-derived neurotrophic factor [BDNF] pDNA). The PCA/Dex nanoparticles conjugated with Arg8, a cell-penetrating peptide that enhances permeability through a round window membrane in the inner ear for gene delivery, exhibited high uptake efficiency in HEI-OC1 cells. This potential carrier co-delivering Dex and the gene into inner ear cells has a diameter of 120–140 nm and a zeta potential of 20–25 mV. Different types of genes were complexed with the Dex-loaded PCA nanoparticle (PCA/Dex/gene) for gene expression to induce additional anti-inflammatory effects. PCA/Dex showed mildly increased expression of GFP and lower mRNA expression of inflammatory cytokines (IL1b, IL12, and INF γ) than did Dex-free PCA nanoparticles and Lipofectamine[®] reagent in HEI-OC1 cells. In addition, after loading Cx26 siRNA onto the surface of PCA/Dex, Cx26 gene expression was downregulated according to real-time polymerase chain reaction for 24 h, compared with that using Lipofectamine reagent. After loading BDNF DNA into PCA/Dex, increased expression of BDNF was observed for 30 h, and its signaling pathway resulted in an increase in phosphorylation of Akt, observed by Western blotting. Thus, Dex within PCA/Dex/gene nanoparticles created an anti-inflammatory effect and enhanced gene expression.

Keywords: cell-penetrating peptide, nanoparticle, dexamethasone, gene delivery, brain-derived neurotrophic factor

Introduction

An inner ear delivery system for drugs (or genes) has been developed using viral or non-viral vectors.¹ Viral vectors have been used to deliver genes due to their high transfection ability.² However, non-viral vectors have been considered as potential carriers due to problems with viral vectors, such as carcinogenesis, immunogenicity, broad tropism, limited DNA packaging capacity, and production difficulty.¹ A non-viral delivery system, a polymer nanoparticle carrier, has been investigated due to its biocompatibility and high stability.³ Nanoparticles offer targeted drug delivery to specific cells.³ Many kinds of nanoparticles including polymersomes,⁴ solid lipid nanoparticles,⁵ and polylysine⁶ have been used as inner ear delivery carriers, and the functionalization of peptide moieties on their surfaces has also been reported to target the special cell populations of the inner ear, such as spiral ganglion neuron and

outer hair cells.^{7,8} However, few peptide moieties used as permeability enhancers for the round window membrane have been reported.

Cell-penetrating peptides (CPPs) have been reported as permeability enhancers for inner ear gene delivery and have been shown to provide high uptake efficiency.^{9,10} In our previous report,¹¹ nanoparticles of PHEA-g-C18-Arg8 (PCA), conjugated to the CPP arginine 8 (Arg8), were synthesized to increase the round window membrane permeability and to target cellular uptake. In that study, a hydrophobic dye, Nile red, and the reporter gene green fluorescence protein (GFP) were loaded onto the core and the surface of the PCA nanoparticle, respectively, and the delivery efficiency to the organ of Corti, modiolus and spiral ligament cells was observed in an *in vivo* study. Although the possibility of Arg8 as a permeability enhancer was evaluated through the round window membrane,¹¹ three kinds of CPPs (Penetratin, Tat, and Arg8) were compared as inner ear delivery enhancers.^{12,13} Dexamethasone (Dex), a type of steroid, has been reported to have transient dilatatory effects on nuclear pores, expanding up to 135 nm in diameter.^{14,15} Therefore, the presence of Dex enhances the gene transfection efficiency in cells, where Dex binds to the glucocorticoid receptor in the cytosol,^{16–18} and confers protective effects on cochlear cells against inflammation in the inner ear, such as sudden sensorineural hearing loss through its anti-inflammatory effects.¹⁹

Thus, the loading of Dex inside the PCA nanoparticle (PCA/Dex) may increase gene expression by expanding the nuclear pore and reducing inflammation in the inner ear. Therefore, the co-delivery effect of the PCA/Dex nanoparticle system with RNA or DNA was investigated by encapsulating both Dex and genes (siRNA or DNA). In the PCA/Dex nanoparticle, we incorporated connexin 26 (Cx26) siRNA, as it is commonly involved in congenital deafness,²⁰ while for hearing restoration and neural regeneration, brain-derived neurotrophic factor (BDNF) DNA was applied.²¹

Materials

Polysuccinimide (PSI) was synthesized as reported previously.²² Octadecylamine (C18), ethanolamine, 1,6-hexanediamine, Dex, and 4-(*N*-maleimidomethyl)cyclohexane carboxylic acid *N*-hydroxysuccinimide ester (SMCC) were purchased from Sigma-Aldrich (St Louis, MO, USA). Arg8 (RRRRRRRR), Penetratin (RQIKIWFQNRRMKWKKK) and Tat (GRKKRRQRRPPQC) conjugated with rhodamine were purchased from Pepton (Daejeon, South Korea). GFP DNA was a fragment

containing CMV promoter and GFP CDS from pEGFP-C2 purchased from Invitrogen, Inc. (Carlsbad, CA, USA). BDNF DNA was a pCMV6-BDNF plasmid purchased from Addgene (Cambridge, MA, USA). The solvents *N,N*-dimethylformamide (DMF) and dimethyl sulfoxide (DMSO) were purchased from Sigma-Aldrich.

Methods

CPP screening

HEI-OCI cell culture

The cell uptake and cytotoxicity of CPPs were assessed using the immortalized mouse organ of Corti cell line HEI-OCI, provided by Dr MK Park (Seoul National University, College of Medicine, Seoul, South Korea). HEI-OCI cells were grown and passaged in Dulbecco's Modified Eagle's Medium, supplemented with 10% fetal bovine serum and 50 U/mL recombinant mouse interferon- γ , and then cultured in a humidified 10% CO₂ environment at 33°C.

Cytotoxicity test of CPPs in HEI-OCI cells

The cytotoxicity of Penetratin, Tat, and Arg8 against HEI-OCI cells was examined as follows. HEI-OCI cells were plated in 96-well plates at a density of 1×10^4 /well in 0.1 mL complete growth medium and incubated to 80% confluence for 24 h. The cells were then treated with Penetratin, Tat, and Arg8 peptides conjugated with rhodamine and DMSO as a vehicle for 24 h. Cell viability was determined using a commercially available 3-(4,5-dimethylthiazol-2-yl)-2,5-diphenyltetrazolium bromide (MTT) assay according to the manufacturer's protocol (EZ-Cytox; Daeil Lab, Seoul, South Korea). After incubation, the optical densities of the samples were determined at 450 nm using a microplate reader (Bio-Rad Laboratories, Hercules, CA, USA).

Cellular uptake test of CPPs in HEI-OCI cells

HEI-OCI cells were plated on a Lab-Tek™ II Chamber Slide™ System (Nunc, Roskilde, Denmark) and treated with Penetratin, Tat, and Arg8 peptides conjugated with rhodamine for 4 and 8 h at the maximal safe dose as determined by a cytotoxicity test. Cells were fixed with 4% paraformaldehyde solution and mounted with Vectashield Mounting Medium and DAPI (Vector Laboratories, Burlingame, CA, USA). The treated cells were observed under a confocal microscope (LSM5 Live Configuration Variotwo VRGB; Zeiss, Jena, Germany) and a fluorescence-activated cell sorter (FACS, BD FACS Canto™ II; Becton Dickinson and Company, Franklin Lakes, NJ, USA).

CPP nanoparticle preparation and DEX loading study

Synthesis of PCA nanoparticles

PCA nanoparticles were synthesized as reported previously.¹¹ Briefly, PSI was dissolved in DMF at a concentration of 138.6 mg/mL, and C18 was dissolved in DMF at 70°C. The hydrophobic conjugation reaction was performed by adding the C18 solution to the PSI solution and allowing to react at 70°C for 24 h. Ethanolamine was added in a dropwise manner to the PSI-g-C18 solution and allowed to react at room temperature for 24 h. The mixture was added to DMF solution containing 1,6-hexanediamine and stirred at 70°C for 24 h (PHEA-g-C18-NH₂). PHEA-g-C18-maleimide (PHEA-g-C18-M) was prepared by reacting PHEA-g-C18-NH₂ with SMCC. Finally, the PHEA-g-C18-M mixture and cysteine-terminated Arg8 peptide powder were mixed in phosphate-buffered saline (PBS) buffer (pH 7.4) and incubated at room temperature for 24 h.

Characterization of nanoparticles

The self-assembly behavior of PCA was characterized by the critical micelle concentration (CMC), which was determined using pyrene as the fluorescent probe. The fluorescence emission spectrum of pyrene (6×10⁻⁴ M) was recorded at 390 nm in the PCA concentration range of 10⁻³ to 3 mg/mL. The excitation wavelength was 300–360 nm, and the slit openings for excitation and emission were set at 2.5 nm. The intensity ratios of the peaks at 333 and 337 nm (I₃₃₇/I₃₃₃) were plotted to determine the CMC. Nanoparticle size and zeta potentials were analyzed using dynamic light scattering measurements (Zetasizer Nano ZS90; Malvern, Worcestershire, UK).

Drug loading and release study

Dex (Sigma-Aldrich)-loaded PCA nanoparticles (PCA/Dex) were prepared using a standard dialysis technique. In brief, the PCA copolymers (30 mg) and Dex (6 mg) were dissolved in DMSO (2 mL). After Dex was loaded into the PCA nanoparticle, the nanoparticles were purified by dialysis using a dialysis membrane (MW 6,000–8,000) against deionized water. The Dex loading ratio of the PCA nanoparticle was measured as described in our previous study.¹¹ The release rate of Dex from the PCA nanoparticle was examined in a simulated perilymph environment as a reference.^{11,23} Each sample solution was collected, 1 mL of 50% ethanol was added, and the amount of released Dex was quantified at 240 nm on an ultraviolet spectrometer in triplicate.

Co-delivery study of DEX and gene-loaded PCA nanoparticles

Determination of the GFP DNA loading ratio

GFP DNA/PCA complexes were prepared at different DNA/micelle weight ratios (w/w) ranging from 0.04 to 0.1. The complexes were gently mixed and incubated for 30 min at room temperature to induce the nanocomplex formation. The nanocomplex was visualized by agarose electrophoresis and the ChemiDoc Imaging system (ChemiDoc™ XRS+, Bio-Rad Laboratories). Moreover, after applying GFP DNA/PCA complexes to the HEI-OC1 cells for 24 h, the fluorescence intensity was analyzed using FACS. For particle visualization using a 120 kV Bio-Transmission Electron Microscope (JEM-1400 plus, JEOL, Tokyo, Japan), 5 μL of sample was deposited onto a discharged copper grid with continuous carbon film and left to adsorb for 60 s. The grid was negatively stained with 3–5 drops of 1% uranyl acetate solution for 30 s. Excess solution on the grid was blotted using a piece of filter paper, and the grid was left to air-dry.

Synergistic effect of Dex on gene delivery

In the presence or absence of Dex, the gene delivery efficiency of the PCA nanoparticle was evaluated and compared with that of the Lipofectamine® control. HEI-OC1 cells treated with PCA/Dex/GFP DNA, PCA/GFP DNA, or Lipofectamine/GFP DNA were analyzed using FACS. To compare the levels of inflammatory cytokines after treatment of these particles, total RNA was isolated from the HEI-OC1 cells using the NucleoSpin® RNA II kit (Macherey-Nagel, Düren, Germany). cDNA was synthesized using Reverse Transcriptase Premix (Elpis Biotech, Daejeon, Korea) and was amplified via polymerase chain reaction (PCR) using Power SYBR® Green Master Mix (Applied Biosystems, Foster City, CA, USA) with gene-specific primer sets. Quantitative real-time PCR (RT-PCR) was performed using the ABI 7500 FAST instrument (Applied Biosystems). The relative levels of mRNA were normalized to levels of GAPDH.

Functional application of DNA and siRNA

Cx26 siRNA downregulation study

Cx26 siRNA tagged with TAMRA and PCA/Dex nanoparticles formed a nanocomplex at a 0.04 weight ratio (siRNA/PCA nanoparticles). To investigate the downregulation of Cx26 mRNA, quantitative RT-PCR was performed at 16 and 24 h after treatment with Lipofectamine® RNAiMax

Table 1 Oligonucleotide sequences used for siRNA and real-time PCR

Gene	Sequence
Cx26 siRNA	Fwd: AAGUUCAUGAAGGGGAGAGAUATT Rev: UAUCUCUCCCUUCAUGAACUU
Cx26	Fwd: TCTGGCTCACTGTCCTCTTC Rev: ATGATCAGCTGCAGAGCCCA
IL1b	Fwd: TGAAGCTGATGGCCCTAAACA Rev: GTAGTGGTGGTCGGAGATTTCGTA
IL12	Fwd: TCCAGTTTCATAGTCCGTGTTACTG Rev: TGAACGTATGCGGAAGTGAAGA
IFN γ	Fwd: GCTACACACTGCATCTTGCTTT Rev: AATGACTGTGCCGTGGCAGTAA
GAPDH	Fwd: TGCAGTGGCAAAGTGGAGATT Rev: CGTGAGTGGAGTCATACTGGAACA

Abbreviation: PCR, polymerase chain reaction.

(Invitrogen) using *Cx26*-specific primers (Table 1). Cellular uptake of *Cx26* after 24 h of treatment in the HEI-OC1 cells was compared with that of Lipofectamine RNAiMax (Invitrogen) using confocal microscopy.

BDNF expression by Western blotting

HEI-OC1 cells were transfected with the PCA/Dex/BDNF DNA complexes for 18, 24, and 30 h. Cell lysates were prepared using RIPA buffer (20 mM Tris-HCl, pH 7.4, 0.01 mM EDTA, 150 mM NaCl, 1 mM PMSF, 1 μ g/mL leupeptin, and 1 mM Na₃VO₄) and resolved by sodium dodecyl sulfate-polyacrylamide gel electrophoresis (SDS-PAGE). Equal amounts of proteins were electroblotted onto a nitrocellulose membrane and then incubated with primary antibodies against pAkt, Akt (Cell Signaling Technology, Danvers, MA, USA), BDNF, GAPDH (Abcam, Cambridge, UK), and horseradish peroxidase-conjugated anti-rabbit IgG (Invitrogen). Positive bands were visualized and analyzed using the ChemiDoc XRS Image system (Bio-Rad Laboratories).

Results

CPP screening

Figure 1 shows the viability, determined by MTT assay, of HEI-OC1 cells treated with each CPP at various concentrations. The biocompatibility of Penetratin and Arg8 with the cells was limited to a dose of 0.025 mg/mL for 24 h and that of Tat to a dose of 0.05 mg/mL. Therefore, the concentration of the peptides used was 0.025 mg/mL in this study. Figure 2A shows a quantitative determination of CPP uptake by flow cytometry using different incubation times (4 and 8 h). In flow cytometric analysis, the cells treated with rhodamine-labeled Arg8 displayed 29.9 \pm 6.6-fold higher fluorescence intensities than that of the control cells, while Penetratin and Tat showed 1.6 \pm 0.1- and 1.9 \pm 0.3-fold higher fluorescence intensities, respectively. Thus, the intensity of Arg8 fluorescence was 18.8 \pm 3.2-fold higher compared with that of Penetratin and 16.1 \pm 1.3-fold higher compared with that of Tat. The visualization of cellular uptake by confocal laser microscopy indicated that all CPPs were abundant in HEI-OC1 cells, but no significant difference was observed between the 4 and 8 h time points (Figure 2B).

Dex release from PCA nanoparticles

Figure 3 shows that the CMC of the PCA nanoparticles was 0.013 mg/mL. In the cell experiments, we selected a PCA concentration higher than the CMC. The percentage of Dex loading was 16.8% \pm 3.2% in the PCA nanoparticle, and the Dex release test was conducted in the artificial perilymph environment (pH 7.4). As shown in Figure 4, PCA/Dex nanoparticle displayed burst release within 1 h. This can be explained that Dex attached on the surface of the PCA nanoparticle was released. After 1 h of release time, sustained release of Dex was shown over 5-d study. This conjectured that the sustained release pattern was from the C18 core of the PCA.

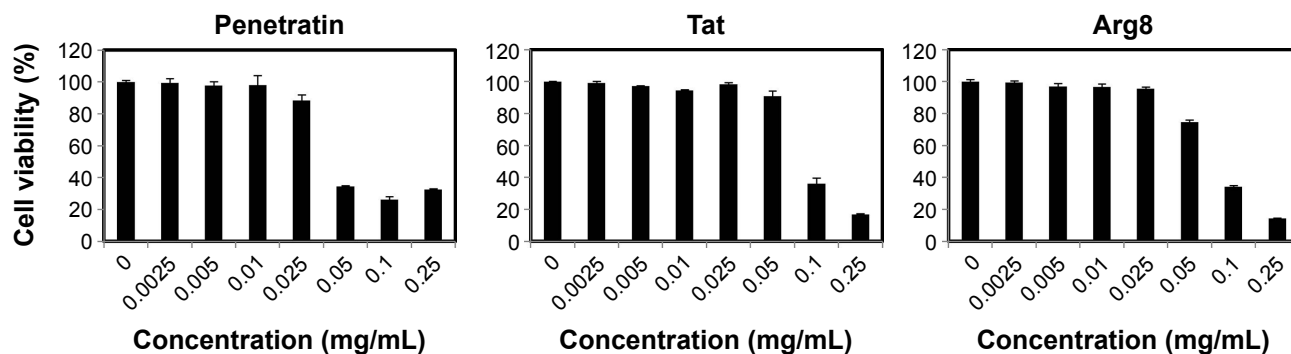


Figure 1 Cytotoxicity of cell-penetrating peptides (Penetratin, Tat, and Arg8) conjugated with rhodamine in the HEI-OC1 cell line (n=3, mean \pm standard deviation).

Note: Cells were treated with the peptides for 24 hours.

Abbreviation: Arg8, arginine 8.

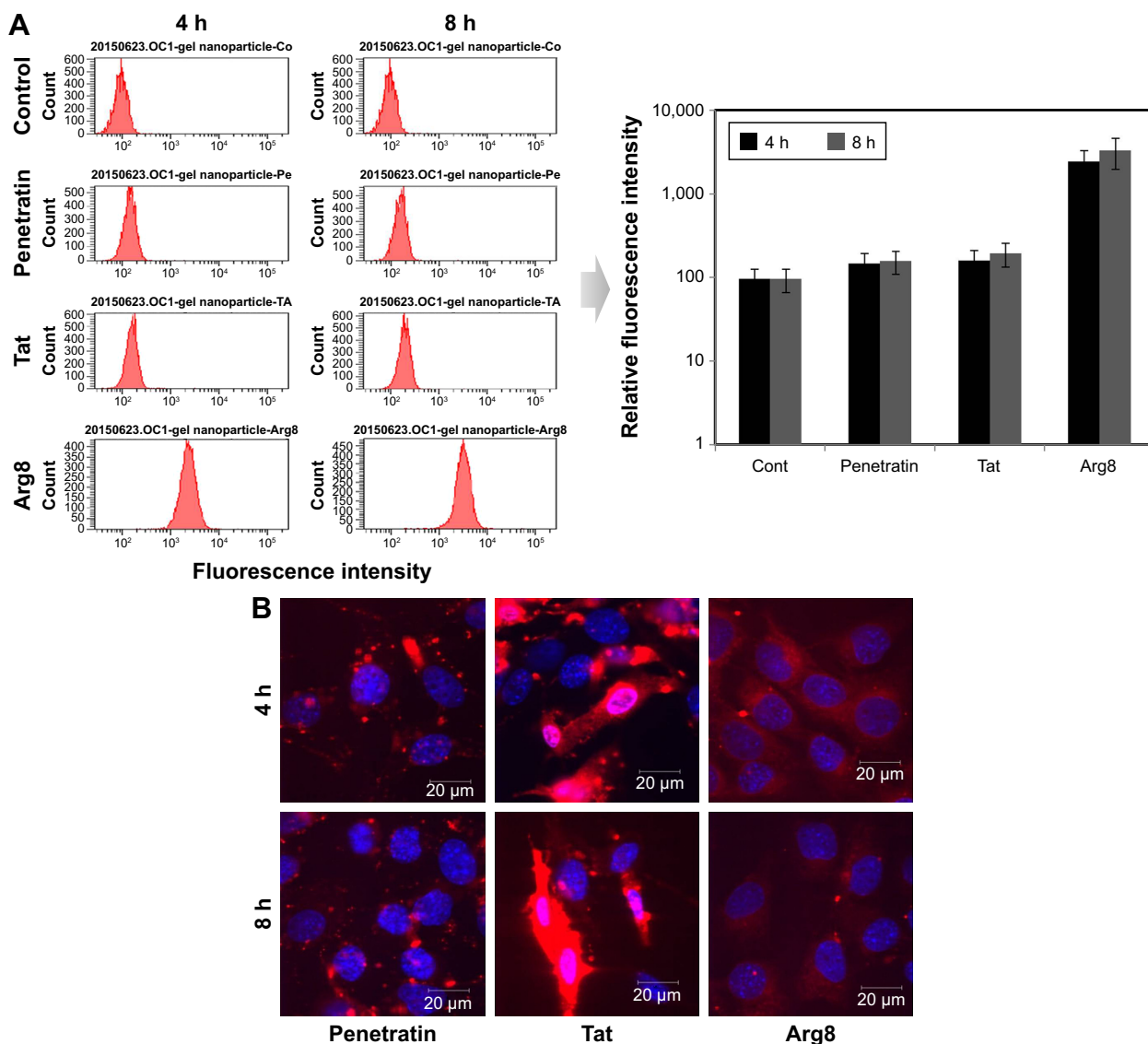


Figure 2 Uptake study of cell-penetrating peptides (Penetratin, Tat, and Arg8; 0.025 mg/mL) into HEI-OC1 cells at 4 and 8 h. **Notes:** All peptides were conjugated with rhodamine (red). **(A)** Fluorescence intensity investigation through FACS analysis (n=3, mean ± SD). **(B)** Uptake investigation using confocal microscopy. **Abbreviations:** Arg8, arginine 8; FACS, fluorescence-activated cell sorter; h, hours; SD, standard deviation.

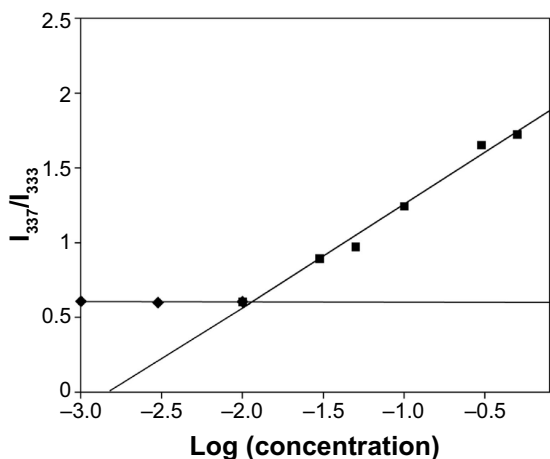


Figure 3 The plot of I_{337}/I_{333} ratio vs log concentration (mg/mL) PCA copolymer. **Abbreviations:** PCA, PHEA-g-C18-Arg8; Arg8, arginine 8.

Co-delivery of Dex and genes

Determination of the GFP DNA loading ratio

Figure 5A shows that the size and zeta potential of GFP DNA/PCA complexes varied with different weight ratios (w/w). The weight ratios of the GFP DNA/PCA complexes used were 0.04, 0.08, and 0.1, while the respective sizes of the complexes were 123.3 ± 0.45 , 138 ± 0.34 , and 143 ± 0.27 nm. The slight increase in size can be attributed to the incorporation of GFP DNA, since the complexes contained the same proportion of C18. The zeta potentials decreased linearly as the DNA weight ratio increased.

Furthermore, Figure 5B shows that the mobility of the PCA nanoparticles was retarded in a dose-dependent fashion by GFP DNA. The GFP DNA bands decreased in mobility

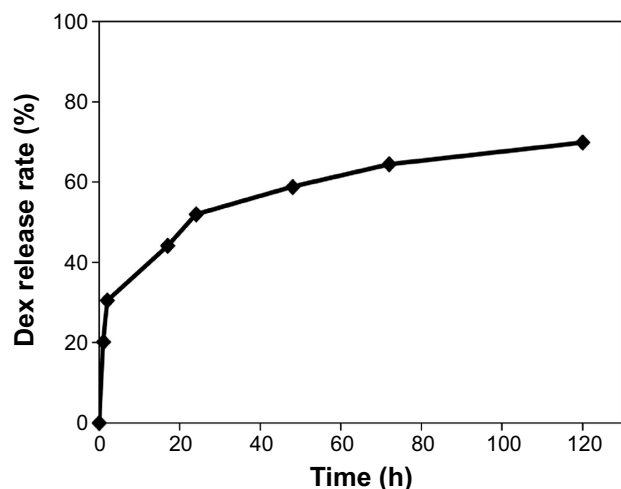


Figure 4 Cumulative amount of Dex released from the PCA/Dex nanoparticle compared with Dex only.

Abbreviations: Dex, dexamethasone; PCA, PHEA-g-C18-Arg8; Arg8, arginine 8; h, hours.

as the weight ratios of GFP DNA/PCA decreased from 0.1 to 0.04. At a weight ratio of 0.1, the band disappeared, but a weak smear was seen.

Figure 6 shows the expression of GFP DNA in HEI-OC1 cells by PCA. The transfection efficiencies were higher than

those of Lipofectamine® 3000 (Lipo), which was used as a positive control. The transfection efficiency increased with the nanoparticle ratio and was 1.5-fold greater at a weight ratio of 0.04 than that of the Lipofectamine group.

Figure 7 shows the morphologies of each nanoparticle incorporated with or without GFP DNA. GFP DNA was observed as fragments on the copper grid, and the PCA was observed as aggregates due to the Arg8 peptide. After the GFP DNA was loaded into the PCA nanoparticle, the PCA/GFP DNA nanoparticles formed spherical structures with an average diameter of 90 nm. Using Bio-TEM, the shape of the GFP DNA-loaded PCA/Dex nanoparticle was also spherical, and the size had increased by 10–20 nm to ~100–110 nm. Since the TEM image showed the dried state of the polymer micelle, the diameter was smaller than the dynamic light scattering result.

Synergistic effect of Dex on gene delivery

After loading the GFP DNA into the PCA/Dex nanoparticles, the GFP DNA at a weight ratio of 0.04 was delivered into HEI-OC1 cells along with the PCA nanoparticles, PCA/Dex nanoparticles, or Lipofectamine. The delivery

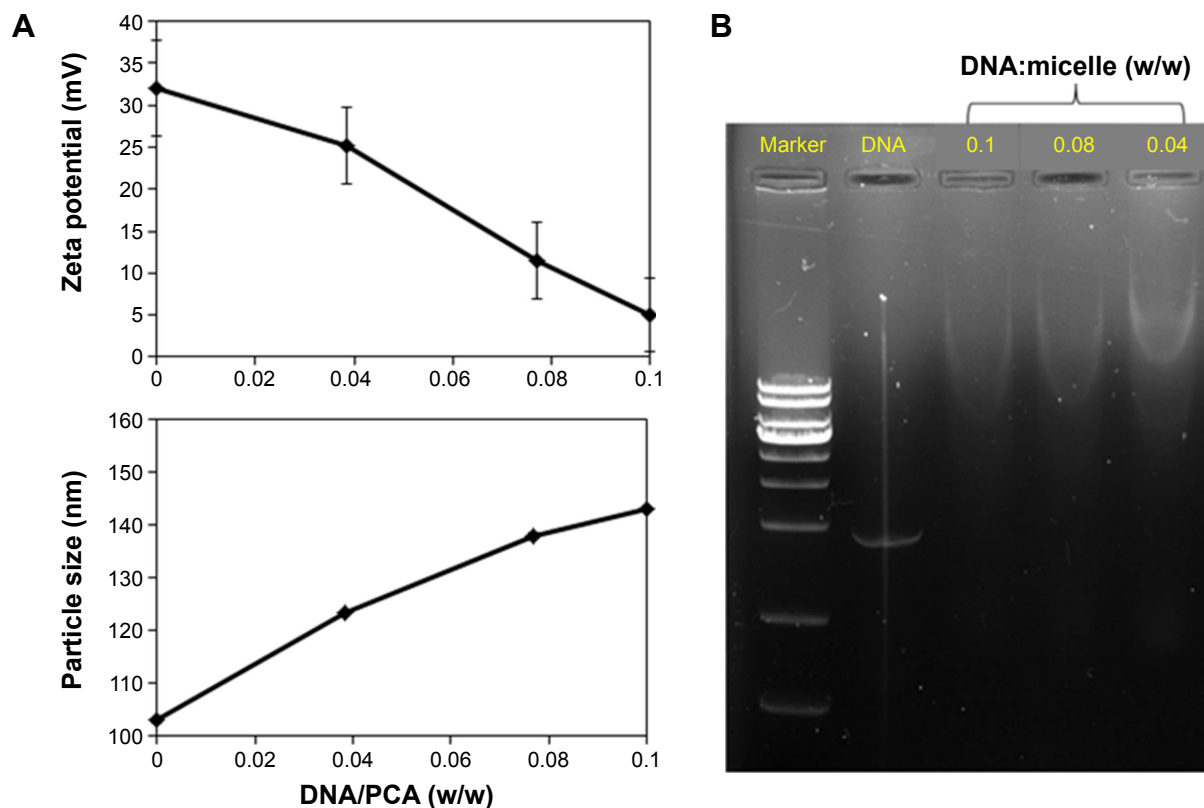


Figure 5 Dynamic light scattering analysis and gel retardation test.

Notes: (A) Zeta potential and particle size analysis of PCA before and after GFP loading, with the weight (μg) ratios of GFP DNA/nanoparticles (w/w; $n=3$, mean \pm SD). (B) Complexation of PCA-GFP polyplexes of different GFP/PCA weight ratios by gel retardation test.

Abbreviations: PCA, PHEA-g-C18-Arg8; GFP, green fluorescent protein; Arg8, arginine 8; SD, standard deviation.

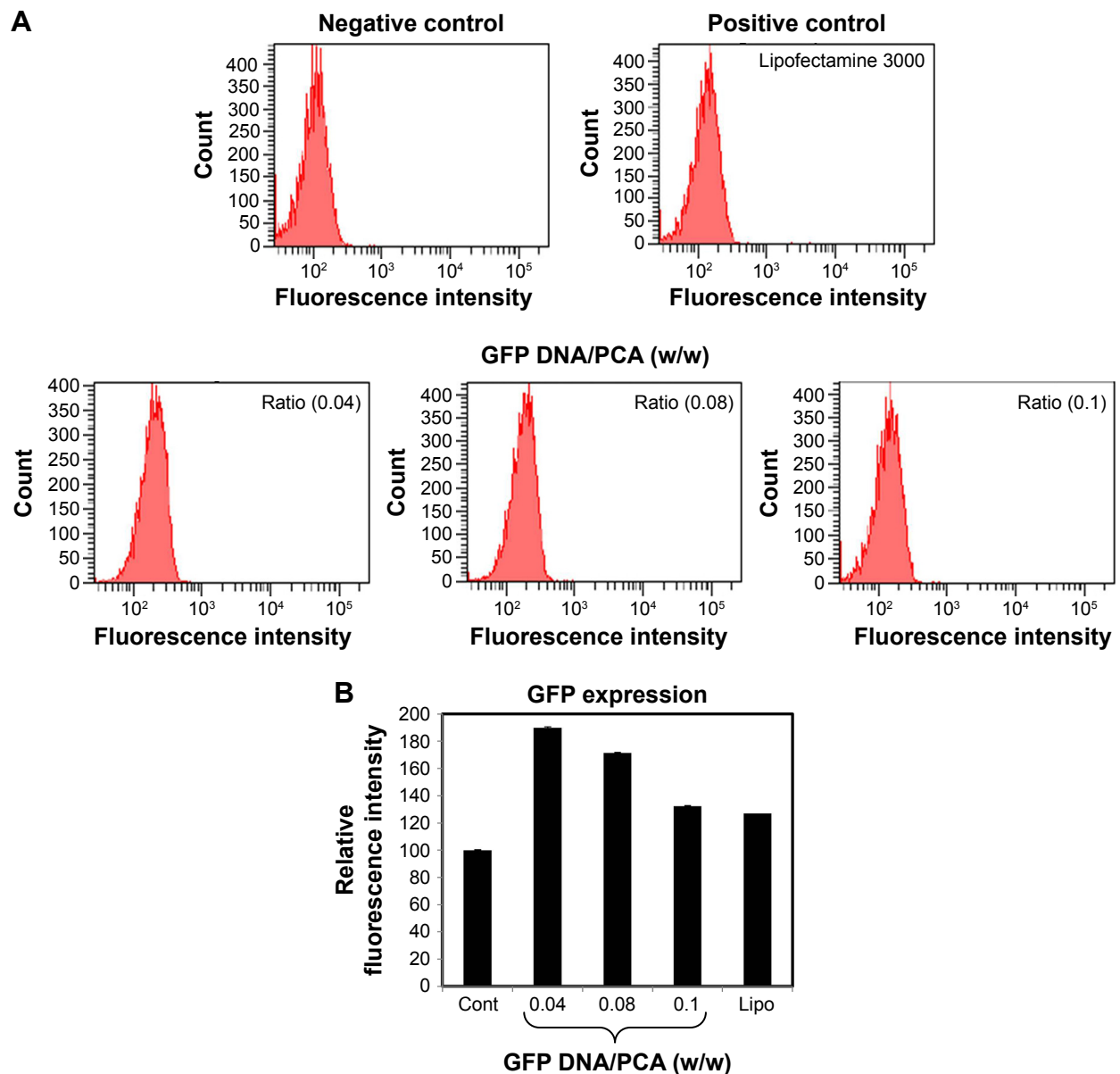


Figure 6 The expression of GFP DNA in HEI-OC1 cells by PCA.

Notes: (A) The expression of GFP DNA by PCA polyplexes (the PCA/GFP weight ratios (w/w) were 0.04, 0.08, and 0.1) at 24 h after delivery into HEI-OC1 cells. (B) Green fluorescence intensity was investigated using FACS analysis (Lipo: Lipofectamine® 3000) (n=3, mean ± SD).

Abbreviations: Arg8, arginine 8; FACS, fluorescence-activated cell sorter; GFP, green fluorescent protein; h, hours; PCA, PHEA-g-C18-Arg8; SD, standard deviation.

efficiency of GFP DNA was validated using FACS. Figure 8 shows that the delivery efficiency of GFP DNA in the Dex group (PCA/Dex/GFP DNA) was mildly increased compared with the Dex-free group (PCA/GFP DNA) in HEI-OC1 cells.

The cellular response of HEI-OC1 cells to inflammation in the presence of PCA/GFP DNA was elucidated. The mRNA levels of IL1b, IL12, and INF γ were measured after culturing the HEI-OC1 cells for 24 h with PCA/GFP DNA with or without Dex. Figure 9 shows that the mRNA levels of the inflammatory cytokines were reduced by Dex-loaded

PCA nanoparticles compared with nanoparticles without Dex. GFP expression in the cells was expressed as the mean fluorescence intensity.

Functional application of DNA and siRNA

Cx26 siRNA silencing

The downregulation efficiency of Cx26 siRNA by TAMRA-loaded PCA/Dex nanopolyplexes was observed by RT-PCR and confocal microscopy. After PCA/Dex/Cx26 siRNA complexes were transfected for 16 and 24 h, the relative mRNA

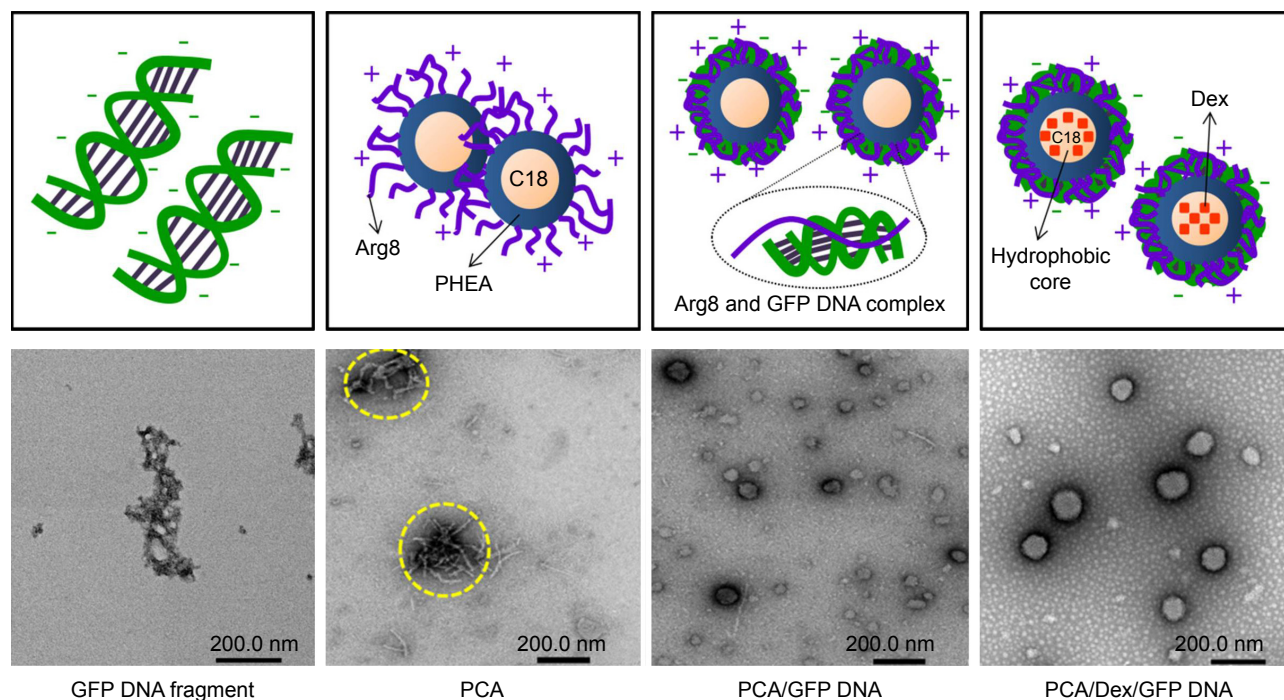


Figure 7 Morphologies of GFP DNA, PCA, PCA/GFP DNA, and PCA/Dex/GFP DNA nanoparticles using 120 kV Bio-TEM. **Abbreviations:** Arg8, arginine 8; Dex, dexamethasone; GFP, green fluorescent protein; PCA, PHEA-g-C18-Arg8.

expression of PCA/Dex/Cx26 was decreased compared with the expression without nanoparticles, with the control or with Lipofectamine RNAiMax (Figure 10A). Although the amount of the Cx26 siRNA-TAMRA loaded into PCA/Dex nanoparticles was 50% less than that using Lipofectamine RNAiMax, the red fluorescence of TAMRA observed in the PCA/Dex nanoparticles was stronger than that using RNAiMax at 24 h, as shown in Figure 10B.

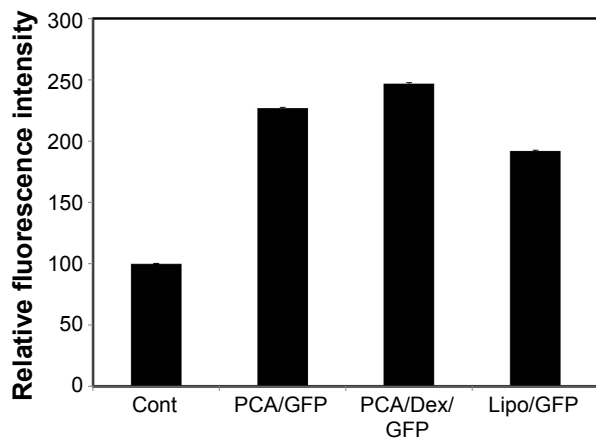


Figure 8 Cellular expression of GFP DNA with PCA (weight ratio: 0.04), PCA/Dex (weight ratio: 0.04) and Lipofectamine® 3000 in HEI-OC1 cells. **Note:** GFP expression intensity in the cells was expressed as the mean fluorescence intensity (n=3, mean ± SD). **Abbreviations:** Arg8, arginine 8; Dex, dexamethasone; GFP, green fluorescent protein; PCA, PHEA-g-C18-Arg8; SD, standard deviation.

The function of BDNF expression in HEI-OC1 cells BDNF reportedly induces phosphorylation of Akt.^{24,25} Figure 11 shows the effect of BDNF expression by PCA/Dex nanoparticles on Akt phosphorylation compared to Lipo, using Western blotting. BDNF expression was observed 18 h after introducing the PCA/Dex/BDNF DNA and Lipo/BDNF DNA. As shown in Figure 11, the BDNF expression rate in the PCA/Dex/BDNF DNA group was increased steadily until 30 h while that in the Lipo/BDNF group was constant. To confirm the functional working of BDNF in the cells, phosphorylation of Akt was monitored. Akt phosphorylation was upregulated 1.83±0.12-fold by PCA/Dex/BDNF DNA at 18 h while 1.49±0.14-fold by Lipofectamine at 24 h and was maintained until 30 h.

Discussion CPP nanoparticles

In this study, the Arg8 peptide was compared with Penetratin and Tat. The zeta potentials of Penetratin, Tat, and Arg8 have been reported to be +8, +9, and +9, respectively.¹² From the CPP screening tests, Arg8 revealed higher cellular uptake despite a similar positive charge density compared with Penetratin and Tat. It has been reported that the uptake efficiency is attributed to the guanidinium head group of the Arg side chain rather than the positive charge alone.^{26,27} The guanidinium group forms bidentate hydrogen bonds with

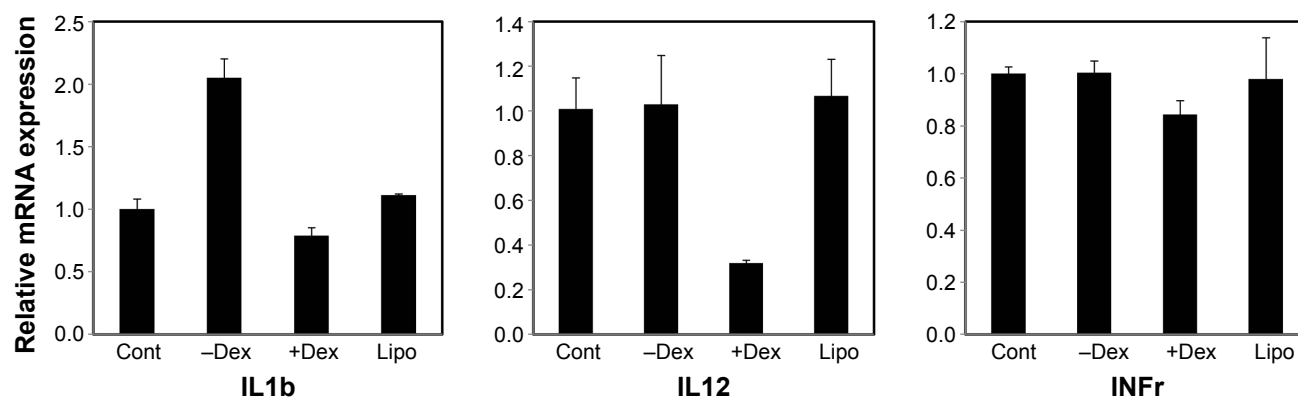


Figure 9 Anti-inflammatory effect of PHEA-C18-Dex-Arg8-GFP in HEI-OC1 cells.

Notes: IL1b, IL12, and INFr expression, as an indication of inflammation, was investigated by RT-PCR in each treatment group (Cont: control group (in HEI-OC1 cells), -Dex: PCA-GFP, +Dex: PHEA-g-C18-Dex-Arg8-GFP, Lipo: Lipofectamine® 3000) 24 h after delivery into HEI-OC1 cells (n=3, mean ± SD).

Abbreviations: Arg8, arginine 8; Dex, dexamethasone; GFP, green fluorescent protein; h, hours; PCA, PHEA-g-C18-Arg8; RT-PCR, real-time polymerase chain reaction; SD, standard deviation.

the negatively charged phosphate, sulfate, and carboxylate groups on the cell surface.²⁶ Therefore, the difference in cell uptake efficiency among Penetratin, Tat, and Arg8 was expected, and the number of Arg amino acids may influence the efficiency of penetration into the cell membrane.²⁸ For this reason, Arg8 was attached to the surface of PHEA-g-C18

nanoparticles. In our previous study, PCA nanoparticles were demonstrated as drug or gene delivery carriers containing hydrophobic dye, Nile red or GFP DNA on the core or surface of the nanoparticles, respectively.¹¹ Loading the gene onto the surface of the nanoparticle can easily lead to degradation by endonucleases, but we considered that intratympanic

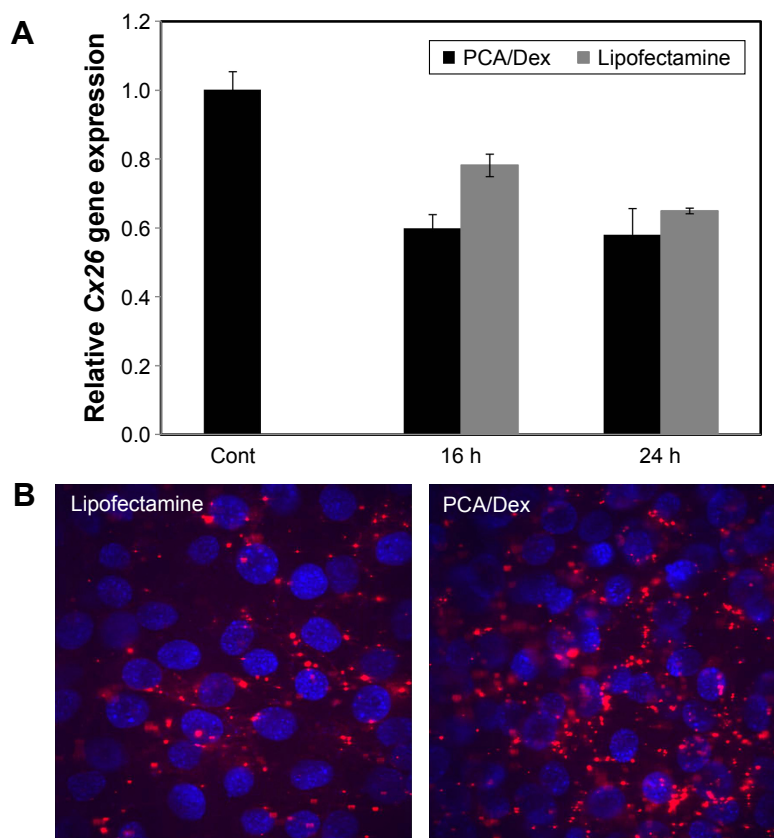


Figure 10 Downregulation effects of Cx26 siRNA cells by PCA/Dex in HEI-OC1 cells compared with Lipofectamine (Lipofectamine® RNAiMax).

Notes: (A) Relative Cx26 gene expression treated with/Cx26 or Lipofectamine/Cx26 with time, according to RT-PCR (n=3, mean ± SD). (B) Cellular uptake of Cx26 siRNA-TAMRA using Lipofectamine or PCA/Dex at 24 h after delivery into HEI-OC1 cells.

Abbreviations: Arg8, arginine 8; Dex, dexamethasone; h, hours; PCA, PHEA-g-C18-Arg8; RT-PCR, real-time polymerase chain reaction; SD, standard deviation.

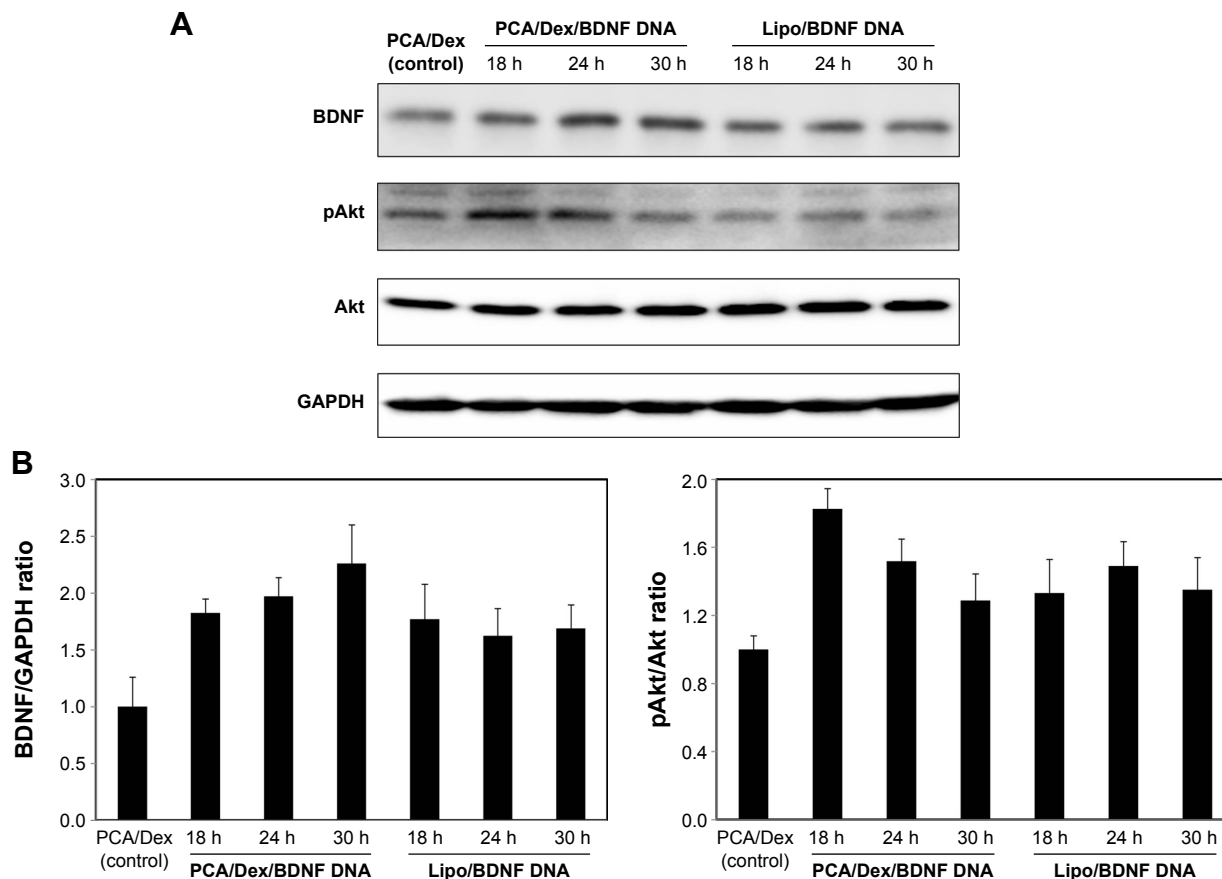


Figure 11 Functional application of PCA/Dex compared with Lipofectamine® 3000 (Lipo) in HEI-OCI cells. **Notes:** (A) After loading PCA/Dex/BDNF DNA and Lipo/BDNF DNA, the expression of BDNF and phosphorylation of Akt were measured by Western blotting. (B) BDNF/GAPDH ratio and pAkt/Akt ratio after normalization against GAPDH (n=3, mean ± SD). **Abbreviations:** Arg8, arginine 8; BDNF, brain-derived neurotrophic factor; Dex, dexamethasone; h, hours; PCA, PHEA-g-C18-Arg8; SD, standard deviation.

local delivery may lower this possibility compared with systemic delivery.

Determination of the GFP DNA loading ratio

When the PCA nanoparticles co-loaded both Dex and the gene, the large accumulation of GFP DNA in the nanoparticles can retard GFP DNA mobility in DLS and the gel retardation test. Figure 5B shows that the migration of the smear decreased as the weight ratio of the GFP DNA in the PCA nanoparticles decreased. This is likely because the positive charges of PCA neutralize the negative charges of the phosphate groups within the GFP DNA backbone. Figure 6 shows the transfection efficiency of each ratio polyplex compared with that of Lipofectamine. The GFP DNA/PCA polyplexes showed higher transfection efficiencies compared with Lipofectamine. Therefore, the polyplex weight ratio was selected as 0.04 for subsequent gene delivery applications. After loading GFP DNA into the PCA nanoparticles, the aggregation bundle of the PCA nanoparticles

was transformed into a spherical shape as shown in Figure 7. This could be attributed to the ionic interaction between the positive charge of the Arg8 peptide at the nanoparticle surface and the negative charge of the GFP DNA. Therefore, it is conjectured that the complexes formed on the nanoparticle surfaces. Even after loading into the PCA/Dex nanoparticles, the shape was also spherical and the particle size increased.

Effect of Dex on gene transfection

First, the synergistic effect of Dex and gene is expected to be increased by the PCA nanoparticle. Dex may induce nuclear pore extension to increase the efficiency of gene transfection. Dex has been reported as a nuclear pore dilatatory factor, and the polyplexes containing Dex showed a 3- to 13-fold higher DNA uptake efficiency in the nucleus, compared with Dex-free polyplexes.²⁹ Therefore, the GFP gene expression level was compared among the PCA/Dex/GFP DNA, PCA/GFP DNA and Lipofectamine groups in Figure 8. The GFP expression level induced by PCA/Dex/GFP DNA

or PCA/GFP DNA was much higher than that induced by Lipofectamine. The GFP expression induced by PCA/Dex/GFP DNA was slightly higher than that induced by PCA/GFP DNA. Since we measured GFP levels using FACS, it is difficult to compare our results with those of Mishra et al,²⁹ who investigated DNA uptake levels in the nucleus. Further study is needed to confirm the effect of Dex on gene delivery via nanoparticles.

Second, the anti-inflammatory effect of Dex via the inhibition of inflammatory cytokines has been investigated. Dex was loaded into the core and the genes (*Cx26* siRNA or BDNF DNA) onto the surface of the PCA nanoparticles. Figure 9 shows an anti-inflammatory effect of Dex-loaded PCA/GFP DNA nanoparticles compared with Dex-free or Lipofectamine. Each inflammatory mRNA, measured in HEI-OC1 cells, decreased in the Dex-loaded PCA nanoparticles compared with nanoparticles containing only genes. In the non-disease state, the inflammatory reaction in the cell itself would occur upon delivery of nanoparticles into the cells. Therefore, Dex reduced the inflammation caused by the gene-loaded nanoparticles.

Third, the function of *Cx26* siRNA and BDNF DNA using the PCA/Dex nanoparticle is shown in Figures 10 and 11. Although *Cx26* gene induces congenital deafness,²⁰ our focus was just to confirm *Cx26* gene downregulation through the function of the *Cx26* siRNA using PCA/Dex. BDNF has been reported to be involved in both the development and maintenance of spiral ganglion neurons.²¹ Furthermore, BDNF is also expressed in hair cells, as well as in the supporting cells of the organ of Corti.²¹ Obviously, damage to hair cells or supporting cells in the auditory epithelium leads to a decrease in BDNF expression, causing degenerative changes in spiral ganglion neurons as well as hearing loss.²¹ Thus, BDNF is a therapeutic candidate for the treatment of deafness.²¹ Figure 11 shows that BDNF was highly expressed by PCA/Dex nanoparticles compared to Lipofectamine. Therefore, the observation of high BDNF expression is important for the recovery of damaged neurons caused by inner ear disease. Akt is representative survival indicator as a serine/threonine kinase that serves as important mediator of various cellular processes.³⁰ It is one of the key downstream mediators of the phosphoinositide-3-kinase (PI3K) signaling pathway, which mediates hair cell survival and leads to activation of Akt by phosphorylation.³¹ BDNF increased the SG neuron survival and neurite formation through phosphorylation of Akt and p38.²⁴ So the phosphorylation of Akt was checked using phosphor-Akt antibody. We are now investigating high gene expression via PCA/Dex

nanoparticles and whether these nanoparticles represent a meaningful therapeutic application in vivo.

Conclusion

PCA/Dex nanoparticles were developed for the delivery of genes to determine synergistic effects of Dex on gene expression. Cationic PCA nanoparticles were self-assembled to create cationic micelles containing C18 core together with loaded Dex and an Arg8 peptide shell for electrostatic complexation with nucleic acids (*Cx26* siRNA, GFP DNA or BDNF pDNA). Dex-loaded polyplexes showed an anti-inflammatory effect, an effect not seen with the Dex-free polyplexes. The gene delivery systems co-loaded with Dex also achieved slightly higher gene expression levels compared with those using Lipofectamine. In summary, Dex in PCA/Dex nanoparticles stabilized the nanoparticles, induced an anti-inflammatory effect, and enhanced gene expression.

Acknowledgments

This research was supported by the Basic Science Research Program through the National Research Foundation of Korea (NRF) funded by the Ministry of Science, ICT and Future Planning (2014R1A1A1002911), as well as by a grant from the E.N.T. Fund of the Catholic University of Korea created in the 2016 program year. This work was supported by the Brain Korea 21 (BK21) Program and in part by the Korea Basic Science Institute (KBSI).

Disclosure

The authors report no conflicts of interest in this work.

References

1. Yin H, Kanasty RL, Eltoukhy AA, Vegas AJ, Dorkin JR, Anderson DG. Non-viral vectors for gene-based therapy. *Nat Rev Genet.* 2014;15(8): 541–555.
2. Jero J, Mhatre AN, Tseng CJ, et al. Cochlear gene delivery through an intact round window membrane in mouse. *Hum Gene Ther.* 2001;12(5): 539–548.
3. Li L, Chao T, Brant J, O'Malley B Jr, Tsourkas A, Li D. Advances in nano-based inner ear delivery systems for the treatment of sensorineural hearing loss. *Adv Drug Deliv Rev.* Epub 2016 Jan 12.
4. Zhang Y, Zhang W, Johnston AH, Newman TA, Pyykko I, Zou J. Comparison of the distribution pattern of PEG-b-PCL polymersomes delivered into the rat inner ear via different methods. *Acta Otolaryngol.* 2011;131(12):1249–1256.
5. Roy S, Glueckert R, Johnston AH, et al. Strategies for drug delivery to the human inner ear by multifunctional nanoparticles. *Nanomedicine.* 2012;7(1):55–63.
6. Zhang W, Zhang Y, Lobler M, et al. Nuclear entry of hyperbranched polylysine nanoparticles into cochlear cells. *Int J Nanomedicine.* 2011; 6:535–546.
7. Zhang Y, Zhang W, Johnston A, Newman T, Pyykko I, Zou J. Targeted delivery of Tet1 peptide functionalized polymersomes to the rat cochlear nerve. *Int J Nanomedicine.* 2012;7:1015–1022.

8. Roy S, Johnston AH, Newman TA, et al. Cell-specific targeting in the mouse inner ear using nanoparticles conjugated with a neurotrophin-derived peptide ligand: potential tool for drug delivery. *Int J Pharm.* 2010;390(2):214–224.
9. Miwa T, Minoda R, Kaitsuka T, Ise M, Tomizawa K, Yumoto E. Protein transduction into the mouse otocyst using arginine-rich cell-penetrating peptides. *Neuroreport.* 2011;22(18):994–999.
10. Dash-Wagh S, Jacob S, Lindberg S, Fridberger A, Langel U, Ulfendahi M. Intracellular delivery of short interfering RNA in rat organ of Corti using a cell penetrating peptide PepFect6. *Mol Ther Nucleic Acids.* 2012;1:e61.
11. Yoon JY, Yang KJ, Kim DE, et al. Intratympanic delivery of oligoarginine-conjugated nanoparticles as a gene (or drug) carrier to the inner ear. *Biomaterials.* 2015;73:243–253.
12. Liu C, Tai L, Zhang W, Wei G, Pan W, Lu W. Penetratin, a potentially powerful absorption enhancer for noninvasive intraocular drug delivery. *Mol Pharm.* 2014;11(4):1218–1227.
13. Liu L, Venkatraman SS, Yang YY, et al. Polymeric micelles anchored with TAT for delivery of antibiotics across the blood–brain barrier. *Biopolymers.* 2008;90(5):617–623.
14. Kastrup L, Oberleithner H, Ludwig Y, Schafer C, Shahin V. Nuclear envelope barrier leak induced by dexamethasone. *J Cell Physiol.* 2006;206(2):428–434.
15. Shahin V, Albermann L, Schillers H, et al. Steroids dilate nuclear pores imaged with atomic force microscopy. *J Cell Physiol.* 2005;202(2):591–601.
16. Harrell JM, Murphy PJM, Morishima Y, et al. Evidence for glucocorticoid receptor transport on microtubules by dynein. *J Biol Chem.* 2004;279(52):54647–54654.
17. Choi JS, Ko KS, Park JS, Kim YH, Kim SW, Lee M. Dexamethasone conjugated poly(amidoamine) dendrimer as a gene carrier for efficient nuclear translocation. *Int J Pharm.* 2006;320(1–2):171–178.
18. Gruneich JA, Price A, Zhu J, Diamond SL. Cationic corticosteroid for nonviral gene delivery. *Gene Ther.* 2004;11(8):668–674.
19. Paulson DP, Abuzeid W, Jiang H, Oe T, O'Malley BW, Li D. A novel controlled local drug delivery system for inner ear disease. *Laryngoscope.* 2008;118:706–711.
20. Kikuchi T, Kimura RS, Paul DL, Takasaka T, Adams JC. Gap junction systems in the mammalian cochlea. *Brain Res Rev.* 2000;32:163–166.
21. Khalin I, Alyautdin R, Kocherga G, Bakar MA. Targeted delivery of brain-derived neurotrophic factor for the treatment of blindness and deafness. *Int J Nanomedicine.* 2015;10:3245–3267.
22. Nakato T, Kusuno A, Kakuchi T. Synthesis of poly(succinimide) by bulk polycondensation of L-aspartic acid with an acid catalyst. *J Polym Sci A Polym Chem.* 2000;38:117–122.
23. Engleder E, Honeder C, Klobasa J, Wirth M, Arnoldner C, Gabor F. Preclinical evaluation of thermoreversible triamcinolone acetonide hydrogels for drug delivery to the inner ear. *Int J Pharm.* 2014;471(1–2):297–302.
24. Mullen LM, Pak KK, Chavez E, Kondo K, Brand Y, Ryan AF. Ras/p38 and PI3K/Akt but not Mek/Erk signaling mediate BDNF-induced neurite formation on neonatal cochlear spiral ganglion explants. *Brain Res.* 2012;1430:25–34.
25. Kim JH. Brain derived neurotrophic factor exerts neuroprotective actions against amyloid β induced apoptosis in neuroblastoma cells. *Exp Ther Med.* 2014;8:1891–1895.
26. Rothbard JB, Jessop TC, Lewis RS, Murray BA, Wender PA. Role of membrane potential and hydrogen bonding in the mechanism of translocation of guanidinium-rich peptides into cells. *J Am Chem Soc.* 2004;126(31):9506–9507.
27. Nakase I, Takeuchi T, Tanaka G, Futaki S. Methodological and cellular aspects that govern the internalization mechanisms of arginine-rich cell-penetrating peptides. *Adv Drug Deliv Rev.* 2008;60(4–5):598–607.
28. Rothbard JB, Kreider E, Van Deusen CL, Wright L, Wylie BL, Wender PA. Arginine-rich molecular transporters for drug delivery: role of backbone spacing in cellular uptake. *J Med Chem.* 2002;45(17):3612–3618.
29. Mishra D, Kang HC, Cho H, Bae YH. Dexamethasone-loaded reconstitutable charged polymeric (PLGA) n-b-bPEI micelles for enhanced nuclear delivery of gene therapeutics. *Macromol Biosci.* 2014;14(6):831–841.
30. Jason SLY, Wei C. Proliferation, survival and metabolism: the role of PI3K/AKT/mTOR signalling in pluripotency and cell fate determination. *Development.* 2016;143(17):3050–3060.
31. Levano S, Bodmer D. Loss of STAT1 protects hair cells from ototoxicity through modulation of STAT3, c-Jun, Akt, and autophagy factors. *Cell Death Dis.* 2015;6:e2019.

International Journal of Nanomedicine

Publish your work in this journal

The International Journal of Nanomedicine is an international, peer-reviewed journal focusing on the application of nanotechnology in diagnostics, therapeutics, and drug delivery systems throughout the biomedical field. This journal is indexed on PubMed Central, MedLine, CAS, SciSearch®, Current Contents®/Clinical Medicine,

Submit your manuscript here: <http://www.dovepress.com/international-journal-of-nanomedicine-journal>

Dovepress

Journal Citation Reports/Science Edition, EMBase, Scopus and the Elsevier Bibliographic databases. The manuscript management system is completely online and includes a very quick and fair peer-review system, which is all easy to use. Visit <http://www.dovepress.com/testimonials.php> to read real quotes from published authors.